# 4-3 Effects of Spread Spectrum Clocking on Measured Noise Spectra

MATSUMOTO Yasushi, ISHIGAMI Shinobu, and GOTOH Kaoru

Spread spectrum clocking (SSC, or clock FM) techniques have been widely used in electronic devices, such as personal computers, to reduce the spectral amplitude of clock harmonics measured in EMI tests. This paper describes how the amplitude reduction caused by SSC is related to clock FM parameters and resolution bandwidth in the spectrum measurement. Since SSC techniques do not reduce the actual power of clock harmonics, the apparent decrease in harmonic spectra must be carefully treated when evaluating the interference potential of harmonics noises to wireless systems.

***Keywords***
Spread-spectrum clock, Dithered clock, Clock FM, Spectrum measurement, Electromagnetic interference

## 1 Introduction

In recent years, many electric appliances have come to be equipped with microprocessors offering a range of additional functions. The clock frequencies of the processors used in personal computers (PCs) have also reached the gigahertz range and are continuing to increase every year. These electronic information devices emit electromagnetic noise in a wide frequency range—up to several gigahertz—and thus stand as potential sources of interference in nearby wireless systems. As shown in Fig. 1, the harmonics of the base clock signals are predominant in the radiation noise emitted by electronic devices in the gigahertz band[1]. Characteristically, the harmonic spectrum is not a line spectrum but instead displays a certain bandwidth. This is a result of the technique used in these devices of intentional modulation of the clock signal frequency (alternately referred to as Spread Spectrum Clock, or SSC; Clock FM; or Dithered Clock). When SSC is used, the bandwidth of the harmonics of the clock signal is broadened, while the peak amplitude of the spectrum is reduced. The SSC technique thus found wide use beginning in the late 1990s in electronic information devices such as PCs, measurement equipment, wireless systems, and in-vehicle electronic devices, as a method of reducing the peak value of the noise spectrum[2]-[6].

When measuring the noise from electronic devices featuring SSC, it should be noted that clock frequency modulation reduces the power

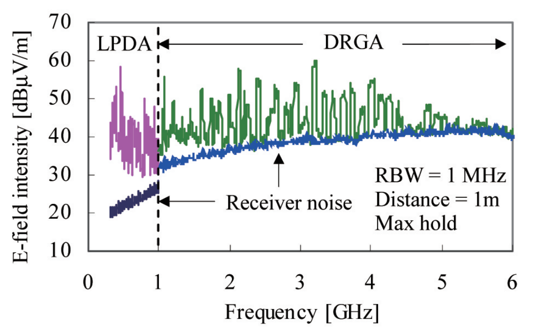


**Fig. 1** Example of PC noise spectrum. Measured at a distance of 1 m using LPDA (Log Periodic Dipole array Antenna) and DRGA (Double Ridged Guide horn Antenna)[1].

spectral density of the harmonics of the clock but not the power of the harmonics. In other words, when the emission limit for an electronic device is specified in terms of the peak value of the amplitude spectrum, introducing SSC can increase the power of the harmonics while maintaining the measured noise level within the allowed range. It has also been clarified that reducing the spectral peak values via SSC does not always reduce the effects on wireless systems[7]-[13].

Generally, the spectrum reduction effect by SSC depends on the frequency deviation, modulation frequency, and modulation waveform of the frequency-modulated harmonics. This effect is also significantly influenced by the resolution bandwidth of the receiver. However, these dependent relations given the conditions indicated above have not been formally established. This is because analytical treatment of the spectrum of a signal frequency-modulated with an arbitrary waveform is difficult, because frequency modulation is a nonlinear process. This report describes theoretical estimation of reducing amplitude in the harmonic spectrum caused by SSC, considering finite resolution bandwidths in spectral measurement. Section **2** introduces a mathematical representation of the harmonic spectrum observed with finite frequency resolution and discusses the effects of the frequency modulation parameters. Section **3** shows a simple formula for evaluating the amount of reduction in the harmonic spectrum by SSC.

## 2 Frequency modulation of clock signals and spectra

### 2.1 Frequency-modulated clock signals

Let us denote the fundamental frequency of the periodic clock signal, $u(t)$, as $f_0$. When the clock signal is not frequency-modulated, this signal can be expressed in the following Fourier series.

$$u(t) = \sum_m I_{m0} \exp(j2\pi m f_0 t) \tag{1}$$

Here, $I_{m0}$ is the complex Fourier coefficient for the $m$-th order harmonic. Next, let us assume that the clock signal $u(t)$ is frequency-modulated with the modulating waveform $V(t)$, as in the following equation.

$$f(t) = f_0(1 + \delta V(t)) \tag{2}$$

Here, $\delta\ (1 \gg \delta > 0)$ is the maximum frequency deviation normalized by frequency $f_0$. The range of $V(t)$ is [−1,1], and its period is assumed as $T_{sw}\ (\gg 1/f_0)$. The frequency-modulated clock signal $u_d(t)$ and its spectrum $U_d(f)$ can be obtained by replacing the time $t$ in Equation (1) with $t'$ given by Equation (3).

$$t' \equiv t + \delta \int_{-\infty}^{t} V(\xi)d\xi \tag{3}$$

Here,

$$\int_{t}^{t+T_{sw}} V(\xi)d\xi = 0$$

$$\begin{aligned} u_d(t) &\equiv u(t') \\ &= \sum_{m=-\infty}^{\infty} I_{m0} \exp\left( j2\pi m f_0 \left( t + \delta \int_{-\infty}^{t} V(\xi)d\xi \right)\right) \\ &\equiv \sum_{m=-\infty}^{\infty} I_m(t) = I_0 + \sum_{m=1}^{\infty} 2\,\mathrm{Re}\left(I_m(t)\right) \end{aligned} \tag{4a}$$

$$\begin{aligned} U_d(f) &\equiv \Im\left(u_d(t)\right) \\ &= \sum_m \Im\left(I_m(t)\right) \\ &\equiv \sum_m I_m(f) \end{aligned} \tag{4b}$$

According to Equation (4), the frequency-modulated clock signal $u_d(t)$ is a superposition of frequency-modulated harmonics denoted as $I_m(t)$ with a complex representation. The center frequency of the $m$-th order harmonic $I_m(t)$ is $mf_0$, the modulation waveform is $V(t)$, and the maximum frequency deviation is $m\delta f_0$. As the frequency modulation uses a periodic function $V(t)$ with a period $T_{sw}$, the harmonic spectrum $I_m(f)$ consists of line spectra equally spaced by $f_{sw}(= 1/T_{sw})$. However, in reality, most of the power is concentrated in the range of approximately $2m\delta f_0$ around the center frequency $mf_0$. Thus, within the range of $m$ for which $m\delta f_0 \ll 1$ holds, the overlap between the adjacent harmonic spectra $I_m(f)$ and $I_{m+1}(f)$ is negligible, such that we can focus our discussion on a single harmonic.

It should be noted that the clock signal waveform received by a measuring receiver is affected by transfer function $H_{sys}(f)$, which reflects the characteristics of the clock transmission system and the measurement system. Thus, the clock signal spectrum $U_{rx}(f)$ input to the receiver is generally expressed with the transfer function $H_{sys}(f)$, as in the following equation.

$$\begin{aligned} U_{rx}(f) &= H_{sys}(f)U_d(f) \\ &= \sum_m H_{sys}(f)I_m(f) \end{aligned} \tag{4b'}$$

Equation (4b') shows that the effects of SSC on the harmonic spectrum can be isolated from the effects of the transfer function $H_{sys}(f)$ for evaluation. Thus, our discussion continues under the assumption that the transfer function satisfies $H_{sys}(f) = 1$.

## 2.2 Frequency-swept harmonic spectrum measured with finite frequency resolution bandwidth

Figure 2 shows a block diagram of a spectrum analyzer. When a harmonic $I_m(t)$ is input to the spectrum analyzer, the input signal is band-limited by a band-pass filter with a resolution bandwidth of $B$ and then subject to envelope detection. The spectrum obtained shows the maximum value [peak spectrum $S_{peak}(f)$] or the root-mean-square (rms) value [rms spectrum, $S_{rms}(f)$] of the envelope amplitude as a function of the center frequency $f$ of the filter. Thus, it should be noted that the displayed spectrum differs from the Fourier transform $I_m(f)$ of the input signal $I_m(t)$. Spectrum $S(f)$ measured for the harmonic $I_m(t)$ is expressed as in the following equation.

$$\begin{aligned} S_{peak}(f_c) &= \max\ |I_b(t, f_c)| \\ S_{rms}(f_c) &= \frac{1}{T}\left( \int_{T/2}^{T/2} \frac{|I_b(t, f_c)|^2}{2} dt \right)^{1/2} \\ I_b(t, f_c) &\equiv \int_{-\infty}^{\infty} I_m(t-\tau)h(\tau, f_c)d\tau \\ h(t, f_c) &\equiv h_0(t)\exp(2\pi j f_c t). \end{aligned} \tag{5}$$

Here, $h(t,f_c)$ is the complex impulse response of the band-pass filter with center frequency $f_c$ and bandwidth $B$, and $h_0(t)$ is the complex envelope of $h(t,f_0)$. $I_b(t,f_c)$ is the harmonic band-limited by the filter. $T$ is the integration time for obtaining the rms value and is assumed as sufficiently longer than the modulation period of the harmonic. We denote the harmonic spectrum measured by the spectrum analyzer as $S_{peak}(f)$ or $S_{rms}(f)$ and distinguish this from spectrum $I_m(f)$, which is defined by the Fourier transform.

The convolution integral of Equation (5) can be further processed by the two types of approximation below according to the relationship between bandwidth $B_{sw}$ given by Equation (6) and resolution bandwidth B[14].

$$\begin{aligned} B_{sw} &\equiv (4\delta m f_0 / T_{sw})^{1/2} \\ &= <| dmf(t)/dt |> \end{aligned} \tag{6}$$

Bandwidth $B_{sw}$ corresponds to the square root of the average rate of change in frequency of the harmonic.

(1) When the resolution bandwidth satisfies $B > B_{sw}$

$$\begin{aligned} I_b(t, f_c) &\cong I_m(t-d)H(mf(t-d), f_c), \\ H(f, f_c) &\equiv \Im(h(t+d, f_c)) \end{aligned} \tag{7}$$

Here, $f(t)$ is the frequency change of the clock signal given by Equation (2); $d$ is the transmission delay of the filter; and $H(f,f_c)$ is the Fourier transform of $h(t+d,f_c)$. The ampli-

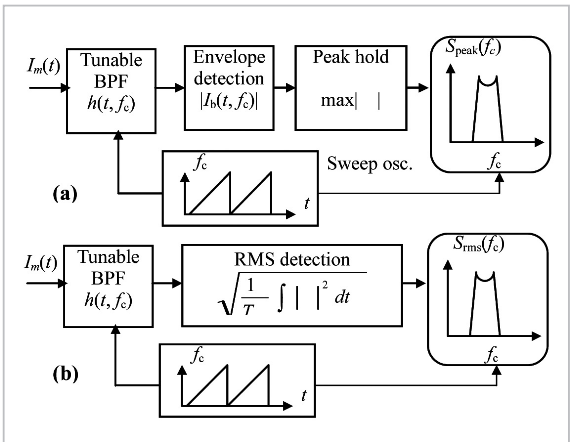


**Fig.2** Block diagram of spectrum measurement using spectrum analyzer

a) Peak spectrum: $S_{peak}(f_c)$

b) rms spectrum: $S_{rms}(f_c)$

tude of the band-limited harmonic changes according to the amplitude of the transfer function of the filter, $|H(mf(t),f_c)|$, at the instantaneous frequency $mf(t)$. A spectrum analyzer is generally designed to display the amplitude accurately for input without frequency modulation at the same frequency as the center frequency $f_c$ of the receiving filter. Thus, we can assume $|H(f_c,f_c)| = 1$.

Therefore, when the approximation (7) holds, then in Equation (5) the maximum amplitude of the envelope of the band-limited harmonic is $\max|I_b(t,f_c)| = |I_{m0}||H(f_c,f_c)| = |I_{m0}|$ for the frequency range of $mf_0(1-\delta)$ to $mf_0(1+\delta)$. This resultant maximum amplitude of the band-limited harmonic is the same as that of the harmonic before band limitation. In other words, SSC has no effect of reduction on the harmonic spectrum $S_{\text{peak}}(f)$ in this case.

(2) When resolution bandwidth satisfies $B \ll B_{sw}$

The convolution integral in Equation (5) can be expressed with the following asymptotic approximation.

$$I_b(t,f_c) \cong \sum_n \left(-jmf'(t_n)\right)^{-1/2} h(t-t_n,f_c) I_m(t_n) \quad (8)$$

Here, $t_n$($n$ is an integer) is the time that satisfies $mf(t_n) = f_c$. According to the approximation (8), the band-limited harmonic can be expressed by applying weighting coefficient $(-jmf'(t_n))^{-1/2}$ to the sequence of the complex impulse response $h(t-t_n,f_c)$ of the filter, generated at each time $t_n$. When the resolution bandwidth $B$ is reduced, the maximum value $h_{max}$ of the envelope amplitude $|h(t)|$ of the impulse response is also reduced. When $h_{max}\,|mf'(t)| \ll 1$ holds, the maximum amplitude of the harmonic spectrum $S_{\text{peak}}(f)$ becomes smaller than $|I_{m0}|$. The reduction in amplitude corresponds to the effect of SSC.

### 2.3 Form of harmonic spectrum

Here, we will examine the example of a clock signal frequency-modulated by a triangular wave with a period of 25 $\mu$s, as shown in Fig. 3a). Many SSC systems use triangular waves for modulation as these waveforms provide greater spectrum reduction than square or sinusoidal waves[2][9]. Figure 3b) shows the peak spectrum $S_{\text{peak}}(f)$ of the harmonic. This spectrum is obtained by a numerical simulation for peak spectra measured by a spectrum analyzer with an ideal Gaussian filter with a bandwidth of 100 kHz. Here, the vertical axis is normalized with the amplitude $|I_{m0}|$ of the harmonic. The harmonic spectrum features a trapezoidal form with quasi-periodic ripples at both edges of the spectrum. An amplitude increase of 5.2 dB at maximum is also observed near the edges of the spectrum as compared with the value at the center frequency $mf_0$ of the harmonic

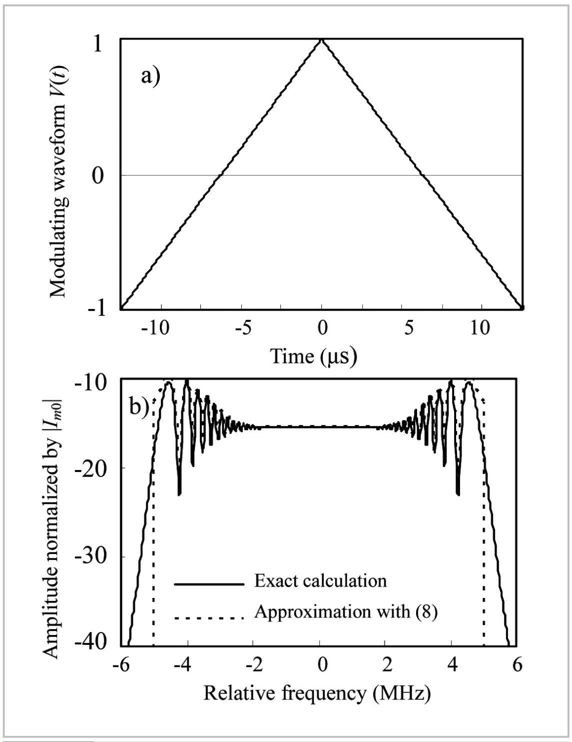


**Fig.3** *Triangular modulation waveform and peak spectrum of FM harmonic (maximum frequency deviation : $m\delta f_0$ = 5 MHz)*

a) Modulation waveform: $V(t)$ ($f_{sw}$ = 40 kHz)
b) Peak spectrum (RBW = 100 kHz)

The characteristics of the spectral form can be explained as follows. In the example indicated in Fig. 3, the receiver filter is a Gaussian filter with a bandwidth $B$ of 100 kHz. The pulse width of the impulse response of this filter is shorter than the modulation period $T_{sw}$ = 25 $\mu$s of the frequency modulation. Thus, when the approximation of Equation (8) is applied, the harmonic $I_b(t)$ band-limited by this filter becomes a sequence of discrete impulse responses, the envelope of which is indicated in Fig. 4c). The impulse responses are generated at the time the instantaneous frequency $mf_0(1+\delta V(t))$ equals the center frequency $f_c$ of the filter. When the center frequency $f_c$ of the filter approaches $mf_0(1+\delta)$ from $mf_0$, the overlap between the adjacent impulse responses grows large, as indicated in Fig. 4b), causing conspicuous interference between these impulses. When the center frequency $f_c$ of the filter is varied, the phase difference $\phi$ between the interfering impulse responses also changes (In the example above, this phase difference is a quadratic function of the center frequency $f_c$) resulting in a change

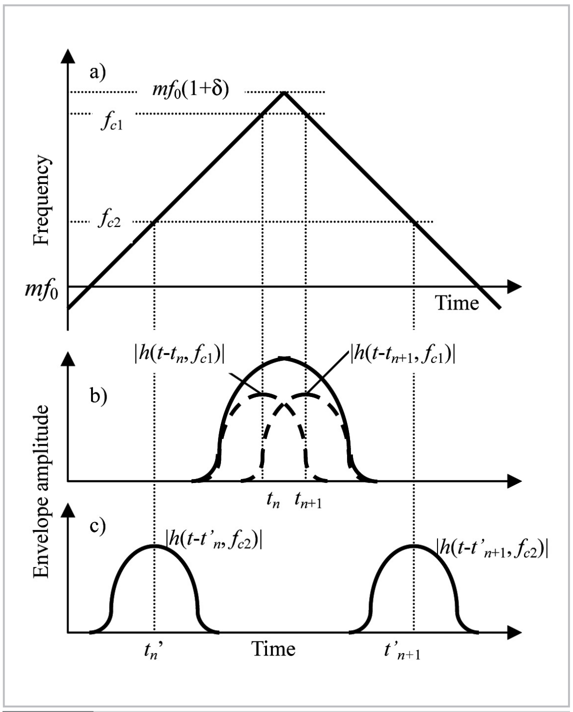


**Fig.4** Band-pass filter output for frequency-modulated harmonic

a) Instantaneous frequency of harmonic: $mf(t)$

b) Envelope amplitude of band-limited harmonic: $|I_b(t, f_{c1})|$. When the center frequency $f_{c1}$ of the filter is close to frequency $mf_0(1+\delta)$ the overlap between the impulse responses, $h(t\text{-}t_n, f_{c1})$ and $h(t\text{-}t_{n+1}, f_{c1})$, is large.

c) Envelope amplitude of band-limited harmonic: $|I_b(t, f_{c2})|$. When the center frequency $f_{c2}$ of the filter is close to frequency $mf_0$ the overlap between the impulse responses can be ignored.

of the maximum amplitude of the envelope. Consequently, the quasi-periodic ripples appear in the spectrum $S_{\text{peak}}(f)$. The amplitude variation in the spectrum is at maximum when the frequency approaches $mf_0(1+\delta)$ and $mf_0(1-\delta)$, because the two adjacent impulse responses overlap almost fully at these frequencies. Figure 3b) compares the spectrum $S_{\text{paek}}(f)$ obtained by an exact computation of Equation (5) with the result of approximation taken from Equation (8). These two values agree well throughout most of the spectrum. These results indicate that Equation (8) serves as an appropriate approximation.

## 2.4 Effects of frequency modulation parameters on the harmonic spectrum

### 2.4.1 *Effects of modulation frequency and frequency deviation*

The reduction in the harmonic spectrum using SSC generally depends on the modulation parameters: frequency deviation, $m\delta f_0$; modulation frequency, $f_{sw} = 1/T_{sw}$; and modulation waveform, $V(t)$. The extent of reduction also depends on the frequency resolution bandwidth $B$ used in spectrum measurement. Here, we will briefly describe the ranges of values for modulation parameters $\delta$ and $f_{sw}$, as used in practical SSC systems. First, the normalized frequency deviation $\delta$ is chosen taking the following issues into consideration.

1) As shown in Equation (8), the harmonic spectrum $S(f)$ decreases in proportion to $m\delta f_0^{-1/2}$. Thus, the frequency modulation effect is larger with a greater value of frequency deviation $\delta$.
2) For the harmonic order $m$ such that the normalized frequency deviation $\delta$ exceeds $2/m$, the major portions of the harmonic spectra $I_m(f)$ and $I_{m+1}(f)$ overlap. As a result, the maximum value of spectrum $S_{\text{peak}}(f)$ increases.
3) When the frequency deviation grows too large, the risk of the loss of clock synchronization increases. In a commercial SSC system, the value of $\delta$ ranges approximately from 0.5 percent to 2 percent[9].

Next, the modulation frequency $f_{sw}$ is determined taking the following issues into consideration.

1) To avoid interference with FM broadcasting, the modulation frequency is set slightly higher than audible frequencies[8][9].
2) As discussed in the previous section, the effect of frequency modulation in the clock appears only when the resolution bandwidth $B$ of the measurement equipment (i.e., of the spectrum analyzer) is smaller than the bandwidth $B_{sw}$ defined in Equation (6). For example, with a value of $\delta$ of 1 percent, $mf_0$ of 1 GHz, and a receiving bandwidth $B$ of 1 MHz, the modulation frequency $f_{sw}$ satisfying this condition is 25 kHz or greater.
3) As discussed below, when the modulation frequency $f_{sw}$ is significantly larger or smaller than the resolution bandwidth $B$, the effect of SSC is reduced.
4) As the modulation frequency increases, it becomes increasingly difficult to generate the frequency-modulated clock strictly in accordance with a desired modulation waveform. This is mainly due to two factors: first, the sampling frequency (which must be sufficiently large relative to modulation frequency) at readout of the modulation waveform data becomes extremely high; and second, the phase noise of the clock increases with an increase in modulation frequency[3].

As indicated in Reference[6], many systems use modulation frequencies within the approximate range of 30 kHz to 50 kHz.

### 2.4.2 Effects of modulation waveform (6)

(1) A modulation waveform that minimizes the spectral peak

When a triangular wave is used as the modulation waveform, the peak spectrum $S_{peak}(f)$ of the harmonic increases at the edge [where the frequency approaches $mf_0(1+\delta)$ and $mf_0(1-\delta)$]. If the derivative $|V'(t)|$ of the modulation waveform is large near the point at which the waveform $V(t)$ is at local maximum or local minimum, the rate of frequency change is also large at the instant the frequency deviation of the harmonic is large. For this reason, and as expected based on Equation (8), the increase in level at the edge of the harmonic spectrum is suppressed. As a result, the harmonic spectrum $S_{peak}(f)$ features a flatter envelope in the major part of the spectrum [from $mf_0(1+\delta)$ to $mf_0(1-d)$] (Figure 5 shows an example), and the maximum value of the peak spectrum becomes smaller.

Reference[8] shows an "optimal" modulation waveform as a polynomial of time, that minimizes the maximum value of the spectrum. However, this waveform is empirically obtained, and the theoretical basis—or method of determination—of the optimal modulation waveform remains unstated. Below, we show the conditions for a modulation waveform that minimize the maximum value of the spectrum $S_{peak}(f)$.

As discussed earlier, the ripple of the peak spectrum $S_{peak}(f)$ of the harmonic can be

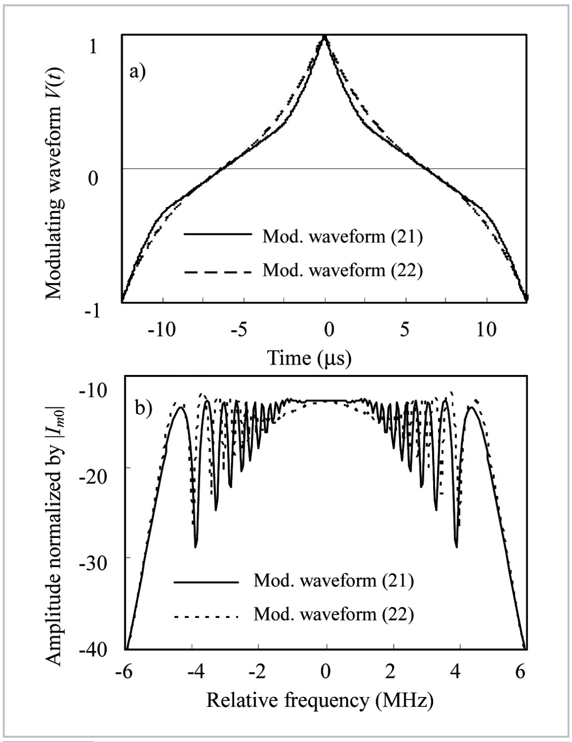


**Fig.5** Modulation waveform and spectrum of frequency-modulated harmonic

a) Modulation waveform (modulation frequency: $f_{sw}$ = 40 kHz)

b) Spectrum: $S_{peak}(f)$ ($m\delta f_0$ = 5 MHz, RBW = 100 kHz) understood as being formed due to in-phase interference between the impulse responses of the filter caused by band-limiting of the frequency-modulated wave. Thus, the maximum amplitude of the peak spectrum can be evaluated as the sum of the envelope amplitudes of the individual impulse responses as derived from Equation (8).

$$\begin{aligned} &S_{peak}(f_{peak}) \\ &\cong \max \sum_n |mf'(t_n)|^{-1/2} |h(t-t_n, f_{peak})| |I_m(t_n)| \\ &= |I_{m0}| \max \sum_n |mf'(t_n)|^{-1/2} h_e(t-t_n) \qquad (9) \\ &h_e(t) \equiv | h(t, f_c) | = | h_0(t) | \\ &mf(t_n) = f_{peak} \end{aligned}$$

Here, $f_{\mathrm{peak}}$ is the frequency at which the spectrum $S_{\mathrm{peak}}(f)$ takes a peak value, and max(*) indicates the maximum value of a variable that is a function of time $t$. Generally, when the frequency $f_{\mathrm{peak}}$ changes, time $t_n$ and $S_{\mathrm{peak}}(f_{\mathrm{peak}})$ also change. If the maximum amplitude given by Equation (9) is constant for different values of the frequency $f_{\mathrm{peak}}$(in other words, if the top of the spectrum $S_{\mathrm{peak}}(f)$ takes a flat envelope), the modulation waveform $V(t)$ can be regarded as optimum. The condition for such a waveform is given by the following equation.

$$\begin{aligned} &S_{peak}(f_{peak}) \\ &= |I_{m0}| \max \sum_n |mf'(t_n)|^{-1/2} h_e(t-t_n) \qquad (10) \\ &= const. \end{aligned}$$

Equation (10) shows that the maximum value of the waveform obtained by summing the envelope amplitude $h_e(t-t_n)$ of the impulse responses with the amplitude weight $|mf'(t_n)|^{-1/2}$ is constant for different values of $f_{\mathrm{peak}}$.

Here, let us add the condition that the rate of frequency change is the same for all values of time that share the same instantaneous frequency. In other words, let us assume

$$|f'(t_0)| = |f'(t_n)| \quad if \quad mf(t_0) = mf(t_n) \qquad (11a)$$

or

$$|V'(t_0)| = |V'(t_n)| \quad if \quad V(t_0) = V(t_n) \qquad (11b)$$

At the least, as shown in Fig. 4c), with small overlap between adjacent impulse responses, the condition given by Equation (11) is considered valid. This is due to the fact that if the rate of frequency change $|f'(t)|$ has different values, the smallest value produces the largest amplitude weight $|mf'(t_n)|^{-1/2}$ in the impulse response, and thus increases the peak of the spectrum $S_{\mathrm{peak}}(f_{\mathrm{peak}})$. In Equation (11), if the center frequency of the filter changes from $f_c$ to $f_c+\Delta f_c$, times $t_1$ and $t_n$ change to $t_0+\Delta t_0$ and $t_n+\Delta t_n$, respectively, to satisfy $f_c+\Delta f_c = mf(t_0)+mf'(t_0)\Delta t_0 = f_c+mf'(t_0)\Delta t_0$ and $f_c+\Delta f_c = mf(t_n)+mf'(t_n)\Delta t_n = f_c+mf'(t_n)\Delta t_n$, respectively. Thus, $f'(t_0) = f'(t_n)(\Delta t_n/\Delta t_0)$ yields the following condition.

$$\begin{aligned} &|V'(t_0)| = |V'(t_n)| \\ &\quad if \ V'(t_0) = \frac{dt_n}{dt_0} V'(t_n) \qquad (12) \\ &\Rightarrow \left| \frac{dt_n}{dt_0} \right| = 1, \quad t_n = \pm t_0 + C \end{aligned}$$

The condition given by Equation (12) shows that the modulation function $V(t)$ is a periodic function and that it is symmetrical in time. As we defined in Equation (2) the period of $V(t)$ as $T_{sw}$ and its range as [−1,1], if we take the initial value of $V(t)$ as $V(0) = 1$, we obtain the following conditions.

$$V(\pm t_0 + kT_{sw}) = V(t_0) \quad (k; \text{integer}) \qquad (13)$$

$$\begin{aligned} &V(0) = 1 \\ &V(T_{sw}/4) = 0 \qquad (14) \\ &V(T_{sw}/2) = -1 \end{aligned}$$

From the periodicity and symmetry we have indicated in Equation (13), the arbitrary time $t_n$ that satisfies $f_p = mf(t_n)$ is expressed with reference time $t_0$ (which varies between 0 and $T_{sw}/2$) and with an integer $k$ as $t_0+kT_{sw}$ or $-t_0+kT_{sw}$. From the conditions in Equation (11), the rate of frequency change $|mf'(t_n)|$ at $t_n$ for an arbitrary $n$ is equal to $|mf'(t_0)|$. These conditions in turn simplify the condition of Equation (10) as follows:

$$|mf'(t_0)|^{-1/2} \max \sum_k (|h(t - t_0 + kT_{sw})| + |h(t + t_0 + kT_{sw})|) = const \quad 0 < t_0 \le T_{sw}/2 \tag{15a}$$

or

$$\begin{aligned} |mf'(t_0)| &= m\delta f_0 |V'(t_0)| \\ &= C \cdot h_m(t_0)^2 \\ h_m(t_0) &\equiv \max \sum_k (|h(t - t_0 + kT_{sw})| + |h(t + t_0 + kT_{sw})|) \end{aligned} \tag{15b}$$

Here, the summation with respect to $k$ in Equation (15) is sufficient if taken for the integer $k$, for which $|h(kT_{sw})|$ is not negligible compared to the maximum value of $|h(t)|$. In the time rage of $0<t<T_{sw}/4$, the modulation waveform $V(t)$ is obtained by solving the first-order differential equation (15) under the conditions given by Equation (14).

$$\begin{aligned} & m\delta f_0 V'(t_0) = C \cdot h_m(t_0)^2 \\ & \quad 0 < t_0 < T_{sw}/4 \\ & V(0) = 1 \\ & V(T_{sw}/4) = 0 \end{aligned} \tag{16}$$

The modulation waveform for other values of time is also obtained easily using the periodicity and symmetry of $V(t)$. The optimal modulation waveform $V(t)$ is obtained using the function $h_m(t)$ defined by Equation (15) as follows.

$$\begin{aligned} V(t) &= 1 - \left( \frac{\int_0^t h_m(t_0)^2 \, dt_0}{\int_0^{T_{sw}/4} h_m(t_0)^2 \, dt_0} \right) \\ & \quad 0 \le t \le T_{sw}/4 \\ h_m(t_0) &\equiv \max \sum_k (|h(t - t_0 + kT_{sw})| + |h(t + t_0 + kT_{sw})|) \end{aligned} \tag{17}$$

Equation (17) gives the optimal modulation waveform if the envelope $h_e(t)$ of the impulse responses of the receiver filter used in the spectrum analyzer is given analytically or numerically. Although the modulation waveform depends on the filter characteristic $h_e(t)$ and modulation frequency $f_{sw}$, this waveform does not depend on the order $m$ of the harmonic nor on the maximum frequency deviation $m\delta f_0$. Thus, as long as overlap of harmonic spectra with adjacent orders can be ignored, the optimal modulation waveform for a certain-order harmonic is optimum for any other harmonics. However, it should be noted that different resolution bandwidths are specified for different measurement frequencies in practical EMI measurement.

(2) Optimum modulation waveform and harmonic spectrum for ideal Gaussian receiver filter

A filter that determines the frequency resolution of a spectrum analyzer generally has a frequency selectivity that can be approximated with a Gaussian filter. Thus, here we postulate an ideal Gaussian filter with a resolution bandwidth of $B$(−3 dB-bandwidth). The transfer function of the filter and the envelope of its impulse response are expressed as follows.

$$\begin{aligned} & H(f, f_c) = \exp\left(-\pi(f - f_c)^2 / B_{imp}{}^2\right) \\ & B_{imp} \equiv \sqrt{\pi/(2\log 2)}B \end{aligned} \tag{18}$$

$$h_e(t) = B_{imp} \exp(-\pi B_{imp}{}^2 t^2) \tag{19}$$

When the resolution bandwidth $B$ is wider than the modulation frequency, the amplitude of the impulse response envelope decays sufficiently in half of the sweep period $T_{SW}$, so it is sufficient to consider only $k = 0$; in other words, only the adjacent impulse responses are included in Equation (17).

$$\begin{aligned} h_m(t_0)^2 &\cong [\max(|h(t - t_0)| + |h(t + t_0)|)]^2 \\ &\cong \begin{cases} \dfrac{B^2\pi}{2\log 2} & \dfrac{\sqrt{2}\log 2}{\pi B} < t_0 \le \dfrac{T_{sw}}{4} \\ \dfrac{2B^2\pi}{\log 2} \exp\left(-\left(\dfrac{\pi B t_0}{\sqrt{\log 2}}\right)^2\right) & 0 \le t_0 \le \dfrac{\sqrt{2}\log 2}{\pi B} \end{cases} \end{aligned} \tag{20}$$

The modulation waveform $V(t)$ is given by the following equation.

$$V(t) = \begin{cases} C'(t - T_{sw}/4) \\ \qquad \dfrac{\sqrt{2}\log 2}{\pi B} < t \le \dfrac{T_{sw}}{4} \\ \dfrac{2C'}{B}\sqrt{\dfrac{\log 2}{\pi}}\, erf\left(\dfrac{\pi B t}{\sqrt{\log 2}}\right) + 1 \\ \qquad 0 \le t \le \dfrac{\sqrt{2}\log 2}{\pi B} \end{cases} \tag{21}$$

$$C' \equiv \left( -\frac{2}{B}\sqrt{\frac{\log 2}{\pi}}\, \mathrm{erf}\left(\sqrt{2\log 2}\right) + \frac{\sqrt{2}\log 2}{\pi B} - \frac{T_{sw}}{4} \right)^{-1}$$

We applied an approximation of $h_m(t_0)$ as $h_e(0)$ for a $t_0$ that satisfies $h_e(-t_0)+h_e(t_0)< h_e(0)$, in order to obtain the analytical form of $V(t)$ as given by Equation (21). When the bandwidth $B$ is wider than $2^{1/2}$ (4 log2)/$\pi$ (or approximately 1.25) times the modulation frequency, this approximation provides sufficient accuracy in practice. As many SSC systems use a modulation period of 20–30 $\mu$s, this application is valid when bandwidth $B$ is approximately 70 kHz or greater. When bandwidth $B$ is narrower, the modulation waveform can be obtained by direct numerical integration of Equation (17).

On the other hand, Reference[8] indicates the equation below as the optimal modulation waveform. We therefore now compare this modulation waveform with the waveform based on Equation (17).

$$V(t) = \begin{cases} -(0.55(t - T_{sw}/4) + 0.45(t - T_{sw}/4)^3) \\ \qquad 0 \le t < T_{sw}/2 \\ (0.55(t - 3T_{sw}/4) + 0.45(t - 3T_{sw}/4)^3) \\ \qquad T_{sw}/2 \le t < T_{sw} \end{cases} \tag{22}$$

Figure 5a) compares the modulation waveform of Equation (21) (with B = 100 kHz) with the modulation waveform given by the polynomial of Equation (22). These waveforms agree well. Figure 5b) shows the results of numerical simulation of the harmonic spectrum $S_{\mathrm{peak}}(f)$ for each modulation waveform. The receiver filter is assumed to be a Gaussian filter with a bandwidth of 100 kHz. The vertical axis is the spectrum $S_{\mathrm{peak}}(f)$ normalized by the amplitude $|I_{m0}|$ of the harmonic [in other words, by the maximum value of the harmonic spectrum $S_{\mathrm{peak}}(f)$ without modulation]. Both modulation waveforms produce mostly flat spectra. The maximum value of the normalized amplitude of the spectrum $S_{\mathrm{peak}}(f)/|I_{m0}|$ is −12.6 dB for Equation (21), and this value is 0.8 dB smaller than the value produced by the polynomial of Equation (22). On the other hand, when the modulation frequency is assumed to be 10 kHz, the modulation waveforms given by Equations (21) and (22) differ as shown in Fig. 6a). As shown in Fig. 6b), the modulation waveform produced by the polynomial of Equation (22) does not result in a flat spectrum, and it cannot be said to be optimum.

Figure 7 compares the modulation waveform $V(t)$, based on Equation (17), obtained for various values of the modulation frequency $f_{sw}$ for a Gaussian filter with a bandwidth of $B$ = 100 kHz. (The figure shows the range

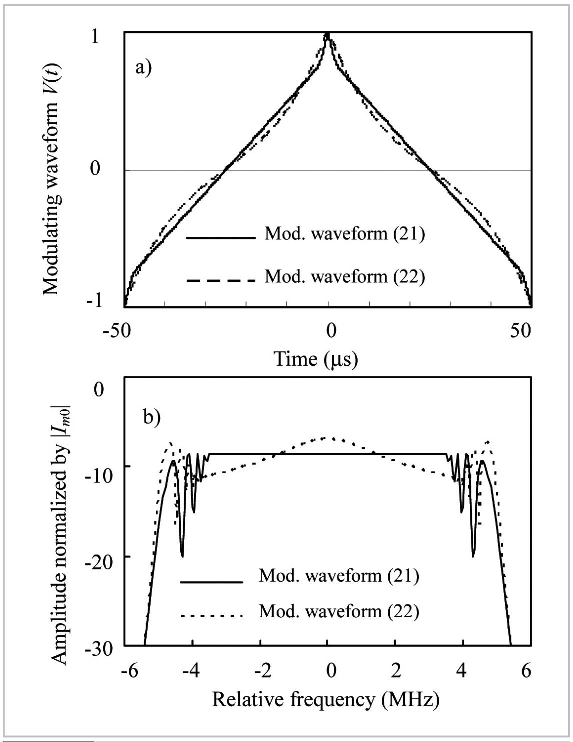


**Fig.6** Modulation waveform and spectrum of frequency-modulated harmonic

a) Modulation waveform (modulation frequency: $f_{sw}$ = 10 kHz)

b) Spectrum: $S_{\mathrm{peak}}(f)$ ($m\delta f_0$ = 5 MHz, RBW = 100 kHz)

$0<t<T_{sw}/4$.) When the modulation frequency is $f_{sw} \gg B$, the optimum modulation waveform has a shape close to that of a triangular wave. This is because the duration of the impulse response with the filter is shorter than the modulation period $T_{sw}$ to a sufficient degree, such that interference between the impulse responses can be ignored most of the time, and hence the function $h_m(t_0)$ takes a nearly constant value [= $\max(h_e(t))$]. Consequently, the modulation waveform becomes a triangular wave with a constant frequency variation rate. On the other hand, when $f_{sw} \ll$ B, the sweep period $T_{sw}$ becomes extremely short relative to the duration of the impulse response. The function $h_m(t_0)$ (for $0<t_0<T_{sw}/2$) then also approaches a constant value that does not depend on $t_0$, and the optimum modulation waveform $V(t)$ asymptotically converges to a triangular wave.

$$\begin{aligned} h_m(t_0) &= \max \sum_{k=-\infty}^{\infty} \left(h_e(t-t_0+kT_{sw}) + h_e(t+t_0+kT_{sw})\right) \\ &\cong 2 \max \sum_{k=-\infty}^{\infty} h_e(t+kT_{sw}) \\ &\cong \frac{2}{T_{sw}} \int_{-\infty}^{\infty} h_e(t)dt \end{aligned} \tag{23}$$

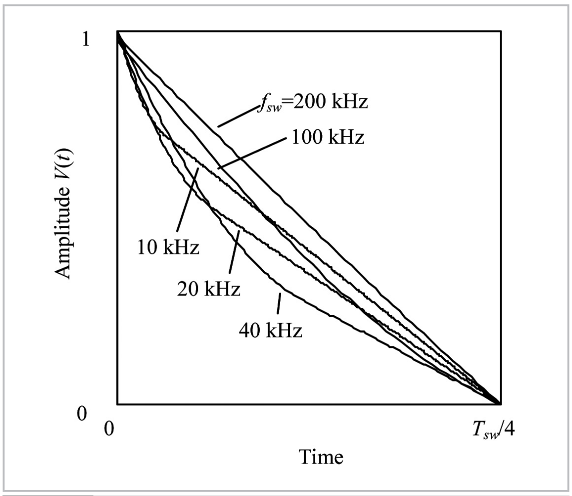


**Fig.7** Comparison between optimum modulation waveforms for different modulation frequencies $f_{sw}$ (RBW = 100 kHz, ideal Gaussian filter). The figure shows a quarter-period of the modulation waveform (0, $T_{sw}/4$).

## 3 Evaluation of the reduction of harmonic spectra by Spread Spectrum Clocking

### 3.1 Investigation of the reduction of spectral amplitude[16]

A peak spectrum $S_{\mathrm{peak}}(f)$ and an rms spectrum $S_{\mathrm{rms}}(f)$ obtained by a spectrum analyzer are given by Equations (4b) and (5). As discussed in Section **2.2**, the convolution integral for acquiring the band-limited waveform $I_b(t)$ of the frequency-modulated harmonic can adopt different approximations according to the frequency change rate $B_{sw}{}^2$ of the harmonic [Equation (6)] and the resolution bandwidth $B$. Here, we investigate the reduction of the spectral amplitude as observed in each case.

(1) Case Ⅰ: $B>B_{sw}$

When the approximation (7) is applied to Equation (5), $S_{\mathrm{peak}}(f)$ and $S_{\mathrm{rms}}(f)$ can be expressed as follows.

$$\begin{aligned} S_{\mathrm{peak}}(f_c) &\cong \max |I_b(t,f_c)| \\ &= |I_{m0}| \max |H(mf(t), f_c)| \\ S_{\mathrm{rms}}(f_c) &\cong \left( \frac{1}{T} \int_{-T/2}^{T/2} \frac{|I_b(t,f_c)|^2}{2} dt \right)^{1/2} \\ &= \frac{|I_{m0}|}{\sqrt{2}} \left( f_{sw} \int_{-Tsw/2}^{Tsw/2} |H(mf(t), f_c)|^2 dt \right)^{1/2} \\ f(t) &\equiv (1+\delta V(t)) f_0 . \end{aligned} \tag{24}$$

As discussed earlier, the filter gain $|H(f_c, f_c)|$ of a spectrum analyzer can be generally regarded to be 1, such that the maximum value of the peak spectrum $S_{\mathrm{peak}}(f)$ equals the amplitude of the input harmonic.

(2) Case Ⅱ: $B \ll B_{sw}$ and $f_{sw} \ll m\delta f_0$

Here, we again indicate the approximation of Equation (8).

$$I_b(t,f_c) \cong \sum_n \left(-jmf'(t_n)\right)^{-1/2} h(t-t_n, f_c) I_m(t_n) \tag{8}$$

Here, $t_n$($n$: integer) is the time that satisfies $mf(t_n) = f_c$. The approximation (8) expresses the waveform produced by applying the weighting coefficient $(-jmf'(t_n))^{-1/2}$ to the sequence of the complex impulse response $h(t-t_n, f_c)$ of the filter generated at time $t_n$. Here, based on the periodicity and symmetry of the modulation waveform $V(t)$ as indicated in Equation (13), it is assumed that an arbitrary time $t_n$ that satisfies $f_p = mf(t_n)$ can be expressed, using reference time $t_0$ (which varies between 0 and $T_{sw}/2$) and the integer $k$, as $t_0+kT_{sw}$ or $-t_0+kT_{sw}$. It is also assumed based on the conditions indicated in Equation (11) that the rate of frequency change $|mf'(t_n)|$ at time $t_n$ is equal to $|mf'(t_0)|$ for an arbitrary $n$. These assumptions hold for modulation waveforms generally used in SSC, such as periodic triangular waves and modified triangular waves. Thus, Equation (8) can be expressed as follows.

$$I_b(t,f_c)=(mf'(t_0))^{-1/2} \sum_k \{ j^{1/2} h(t-t_0-kT_{sw},f_c) I_m(t_0+kT_{sw}) + (-j)^{1/2} h(t+t_0-kT_{sw},f_c) I_m(-t_0+kT_{sw}) \} \quad (25)$$
$$mf(t_0)=f_c \quad (0 \le t_0 < T_{sw}/2).$$

From Equation (25), the envelope amplitude of the band-limited harmonic is given by the following equation.

$$|I_b(t,f_c)| \cong \frac{|I_{m0}|}{B} \left| \sum_k h_e(t-t_0+kT_{sw}) e^{j(\theta+\phi)} + h_e(t+t_0+kT_{sw}) e^{j(\theta-\phi)} \right| \quad (26)$$
$$h_e(t) \equiv |h(t,f_c)|$$
$$\theta \equiv 2\pi(mf_0-f_c)kT_{sw},$$
$$\phi \equiv \pi/4 - 2\pi f_c t_0 + 2\pi m \int_0^{t_0} f(\xi) d\xi.$$

Here, $h_e(t)$ indicates the envelope of the impulse response of the receiver filter $h(t,f_c)$. It should be noted that Equation (26) approximates the rate of frequency change $|mf'(t_0)|$ of the harmonic as the average value, $B_{sw}^2$ [defined by Equation (6)]. This approximation is valid for periodic triangular waves. Equation (26) can be further simplified based on the relationship between the resolution bandwidth $B$ of the spectrum analyzer and the modulation frequency $f_{sw} (= 1/T_{sw})$.

2a) Case IIa: ($B_{sw}^2 = 4m\delta f_0 f_{sw} \gg B^2 \gg f_{sw}^2$)

When the modulation frequency $f_{sw}$ is very small relative to the resolution bandwidth $B$, the duration of the impulse response pulse is much shorter than the modulation period $T_{sw}$, and thus the overlap of the impulse response pulses in Equation (26) can be ignored except for adjacent pulses. Thus, in order to investigate the envelope amplitude of the band-limited harmonic, it is sufficient to consider only a half cycle of the modulation waveform by letting $k=0$ in Equation (26).

$$|I_b(t,f_c)| = \frac{|I_{m0}|}{B_{sw}} \left| h_e(t-t_0) e^{j\phi} + h_e(t+t_0) e^{-j\phi} \right|. \quad (-T_{sw}/4 \le t < T_{sw}/4) \quad (27)$$
$$mf(t_0)=f_c \quad (0 \le t_0 < T_{sw}/4)$$

As the maximum value of the time variation of $|I_b(t,f_c)|$ in Equation (27) corresponds to the peak spectrum $S_{peak}(f_c)$ we can now further investigate the maximum value of this peak spectrum [the maximum value of $S_{peak}(f_c)$ when $f_c$ is varied]. Equation (27) expresses the superposition of two impulse response pulses, $h(t-t_0)$ and $h(t+t_0)$, such that $S_{peak}(f_c)$ takes its maximum value [here $|I_b(t,f_c)|$ is maximum with regard both to time t and to frequency $f_c$] if the following two conditions are satisfied.

1) The peak of the impulse response pulse envelope $h_e(t-t_0)$ overlaps that of the adjacent pulse $h_e(t+t_0)$.
2) The pulses, $h(t-t_0,f_c)$ and $h(t+t_0,f_c)$ interfere in phase.

If we take $t_0 = 0$ in Equation (27), the pulses $h(t-t_0,f_c)$ and $h(t+t_0,f_c)$ overlaps completely, so Condition 1) above is satisfied. However, the phase difference of these pulses is $2\phi = \pi/2$ in this case, in accordance with Equation (26), and Condition 2) is not satisfied. Thus, numerical calculation is generally required to find the maximum value of $S_{peak}(f)$. Nevertheless, we assume the condition $t_0 = 0$, allowing error [$1/\cos(\pi/4)$ (= 3 dB) at maximum] to derive a simple approximate expression. This leads to the approximate maximum value for the peak spectrum $S_{peak}(f)$, as follows.

$$\max(S_{peak}(f_c)) \cong \frac{2|I_{m0}|\cos(\pi/4)\max(h_e(t))}{B} = \frac{\sqrt{2}B_{imp}}{B_{sw}}|I_{m0}| \quad (28a)$$
$$B_{imp} \equiv \max(h_e(t))/|H(f_c,f_c)|$$

Similarly, the maximum value for the rms spectrum can also be expressed as in the following equation.

$$\max(S_{\mathrm{rms}}(f_c)) \cong \frac{2|I_{m0}|\cos(\pi/4)}{\sqrt{2}B_{\mathrm{sw}}}\left(f_{sw}\int_{-\infty}^{\infty}h_e(t)^2\,dt\right)^{1/2} = \frac{|I_{m0}|}{\sqrt{2}}\sqrt{\frac{B_n}{2m\delta f_0}}$$

$$B_n \equiv \frac{\int_0^{\infty}|H(f,f_c)|^2\,df}{|H(f_c,f_c)|^2} = \frac{\int_{-\infty}^{\infty}h_e(t)^2\,dt}{|H(f_c,f_c)|^2}. \quad (28b)$$

Here, the gain of the band-pass filter is assumed $|H(f_c,f_c)| = 1$ at the center frequency. In Equation (28), $B_{\mathrm{imp}}$ and $B_{\mathrm{n}}$ are referred to as the impulse bandwidth and noise bandwidth of the filter, respectively. Generally, $B_{\mathrm{imp}}$ and $B_{\mathrm{n}}$ are on the same order as the resolution bandwidth $B$(−3 dB-bandwidth), such that when $B$ is smaller than $B_{\mathrm{sw}}$ to a sufficient degree, the maximum value of the peak spectrum $S_{\mathrm{peak}}(f)$ is smaller than $|I_{m0}|$, which is the peak spectral amplitude of the harmonic without SSC.

On the other hand, in the rms spectrum [Equation (28b)], when $2m\delta f_0/B_{\mathrm{sw}} = (m\delta f_0/f_{\mathrm{sw}})^{1/2} \gg 1$ holds (in other words, the frequency deviation $\delta f_0$ is much larger than the modulation frequency $f_{\mathrm{sw}}$), $B \ll B_{\mathrm{sw}} \ll 2m\delta f_0$ holds. Thus, the maximum value of the rms spectrum is smaller than without SSC.

2b) Case Ⅱb ($B_{\mathrm{sw}}^2 = 4m\delta f_0 f_{\mathrm{sw}} \gg f_{\mathrm{sw}}^2 \gg B^2$)

When the resolution bandwidth $B$ of the spectrum analyzer is smaller than the modulation frequency, the spectrum analyzer can resolve multiple sidebands (line spectra) with a frequency interval of $f_{\mathrm{sw}}$, which constitutes the Fourier spectrum $I_m(f)$ [Equation (4b)] of the harmonic. In other words, $I_b(t,f_c)$ features a large amplitude only when the center frequency $f_c$ of the filter agrees with one of the sideband frequencies $mf_0+nf_{sw}$ (where n is an integer). Here, the phase term $\exp(j\theta)$, is 1 regardless of the value of the integer $k$. Further, as $f_{\mathrm{sw}} \gg B$ holds, the impulse response duration of the filter is much longer than $T_{\mathrm{sw}}$, and thus the sum with regard to $k$ in Equation (26) can be approximated by the integration of $h_e(t)$.

$$\sum_{k=-\infty}^{\infty}h_e(t \pm t_0 + kT_{\mathrm{sw}})e^{j(\theta\pm\phi)} \cong \frac{e^{\pm j\phi}}{T_{\mathrm{sw}}}\int_{-\infty}^{\infty}h_e(t)dt$$

$$|I_b(t,mf_0+nf_{\mathrm{sw}})| \cong \frac{|I_{m0}||2\cos\phi|f_{\mathrm{sw}}}{B_{\mathrm{sw}}}H_0, \quad (29)$$

$$H_0 \equiv \int_{-\infty}^{\infty}h_e(t)dt$$

From Equation (29), the maximum value of the peak and rms spectra can be expressed as follows.

$$\max(S_{\mathrm{peak}}(f_c)) \cong \frac{2|I_{m0}|}{B_{\mathrm{sw}}T_{\mathrm{sw}}}H_0 = |I_{m0}|\left(\frac{f_{\mathrm{sw}}}{m\delta f_0}\right)^{1/2}H_0 \quad (30a)$$

$$\max(S_{\mathrm{rms}}(f_c)) \cong \frac{|I_{m0}|}{\sqrt{2}}\left(\frac{f_{\mathrm{sw}}}{m\delta f_0}\right)^{1/2}H_0. \quad (30b)$$

(3) Case Ⅲ: Narrow band FM ($m\delta f_0 < f_{\mathrm{sw}}$ or $(B_{\mathrm{sw}}/2)^2 = m\delta f_0 f_{\mathrm{sw}} < f_{\mathrm{sw}}^2$)

Frequency-modulated waves with a modulation index ($m\delta f_0/f_{\mathrm{sw}}$) smaller than 1 are referred to as narrow-band FM signals. In these waves, the carrier component (with a frequency of $mf_0$) constitutes most of the signal power. For this reason, if the center frequency $f_c$ of the spectrum analyzer is set to the center frequency $mf_0$ of the harmonic, the amplitude observed is approximately the same as the amplitude of the harmonic, regardless of the resolution bandwidth. Thus, when the harmonic is a narrow-band FM signal ($m\delta f_0 < f_{\mathrm{sw}}$), the change in the maximum value of the harmonic spectrum due to frequency modulation is negligible.

$$\max(S_{\mathrm{peak}}(f_c)) \cong |I_{m0}|, \quad \max(S_{\mathrm{rms}}(f_c)) \cong |I_{m0}|/\sqrt{2} \quad (31)$$

### 3.2 Simplified evaluation formula for spectrum amplitude reduction

Based on the investigation described in the previous section, we now show a simplified evaluation formula for a reduction in the amplitude of the harmonic spectrum by SSC. Here the modulation waveform is assumed to be a triangular wave, and the band-pass filter of the spectrum analyzer is assumed to be an ideal Gaussian filter with a resolution bandwidth (−3 dB-bandwidth) of $B$. The transfer function and the envelope of the impulse response of this filter are expressed by Equations (18) and (19), respectively. The impulse bandwidth $B_{imp}$ and the noise bandwidth $B_n$ are given by

$$B_{imp} = \sqrt{\pi/(2\log 2)}B,\ B_n = B_{imp}/\sqrt{2}. \quad (32)$$

Figure 8 shows the classification discussed in the previous section. The effects of SSC amplitude reduction on the peak and rms spectra in each case are approximated as follows.

Case Ⅰ ($B^2 \gg B_{sw}^2 \gg f_{sw}^2$):

$$Peak_{SSC}/Peak_{unmod} \cong 1$$

$$RMS_{SSC}/RMS_{unmod} \cong \left(2f_{sw}\int_{f_c-m\delta f_0}^{f_c+m\delta f_0}\frac{|H(f,f_c)|^2}{4m\delta f_0 f_{sw}}df\right)^{1/2} \cong \begin{cases}1 & (B >> m\delta f_0)\\ \sqrt{B_n/(2m\delta f_0)} & (B << m\delta f_0)\end{cases} \quad (33\mathrm{I})$$

Case Ⅱa ($B_{sw}^2 \gg B^2 \gg f_{sw}^2$):

$$Peak_{SSC}/Peak_{unmod} \cong \sqrt{2}B_{imp}/B_{sw}, \quad RMS_{SSC}/RMS_{unmod} \cong \sqrt{B_n/(2m\delta f_0)} \quad (33\mathrm{IIa})$$

Case Ⅱb ($B_{sw}^2 \gg f_{sw}^2 \gg B^2$):

$$Peak_{SSC}/Peak_{unmod} \cong RMS_{SSC}/RMS_{unmod} \cong \sqrt{f_{sw}/(m\delta f_0)}. \quad (33\mathrm{IIb})$$

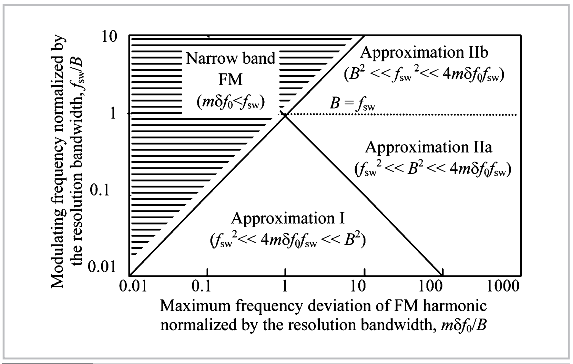


**Fig.8** Conditions of applicable approximations for evaluating effect of clock FM

Case Ⅰ: Approx. Ⅰ($f_{sw}^2 \ll B_{sw}^2 = 4m\delta f_0 f_{sw} \ll B^2$)
Case Ⅱa: Approx. Ⅱa ($f_{sw}^2 \ll B^2 \ll B_{sw}^2$)
Case Ⅱb: Approx. Ⅱb ($B^2 \ll f_{sw}^2 \ll B_{sw}^2$)
Case Ⅲ: Narrow band FM ($m\delta f_0 < f_{sw}$)

Case Ⅲ ($B_{sw}/2 < f_{sw}$):

$$Peak_{SSC}/Peak_{unmod} \cong RMS_{SSC}/RMS_{unmod} \cong 1 \quad (33\mathrm{III})$$

### 3.3 Comparison with results of numerical calculation

To investigate the validity of the simplified evaluation formula, we compared the results obtained by the formula with those of numerical calculations of the convolution integral of Equation (5). Figure 9 shows the dependence of the reduction in peak and rms spectra on the modulation frequency $f_{sw}$ when the resolution bandwidth $B$ is 100 kHz and 1 MHz. Figure 10 shows dependence on resolution bandwidth when the modulation fre-

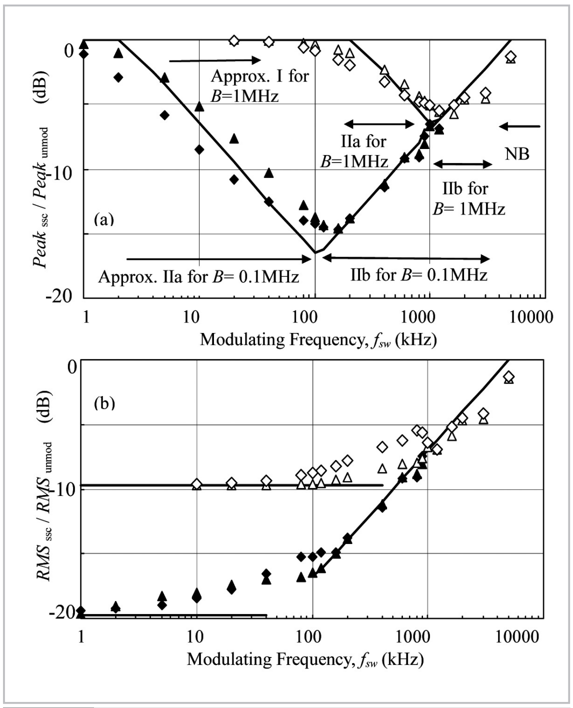


**Fig.9** Results of numerical simulation for amplitude reduction of the harmonic spectrum as a function of modulation frequency $f_{sw}$

a) Peak spectrum
b) rms spectrum
Maximum frequency deviation : $m\delta f_0$ = 5 MHz
Resolution bandwidth, $B$: 1 MHz, 0.1 MHz
Modulation by triangular wave: open (B = 1 MHz) and closed (B = 0.1 MHz) triangles
Modulation waveform by Equation (17): open (B = 1 MHz) and closed (B = 0.1 MHz) rhombuses
Reduction estimated by Equation (33): solid curves

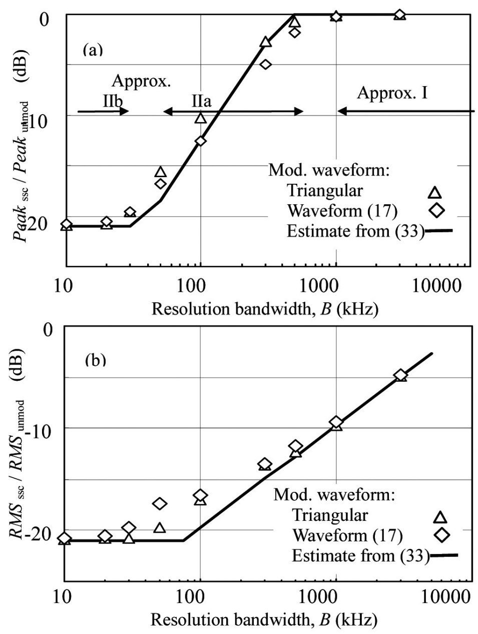


**Fig.10** Dependence of amplitude reduction of harmonic spectrum on resolution bandwidth (results of numerical simulations)

Maximum frequency deviation : $m\delta f_0 = 5$ MHz
Modulation frequency: $f_{sw} = 40$ kHz

quency is 40 kHz. The modulation waveforms used are of two types: triangular waveform, and waveforms produced according Equation (17). Both figures show that Equation (33) provides good approximation for the reduction in spectrum amplitude. As shown in Fig. 9, it is clear that the amplitude of the peak spectrum is most reduced when the modulation frequency $f_{sw}$ is approximately the same as the impulse bandwidth.

## 4 Conclusions

We conducted theoretical analyses of the effects of frequency modulation of clock signals (such as a Spread Spectrum Clock, or SSC), a method widely used in diverse electronic devices such as personal computers (PCs), on the measured harmonic noise spectrum. As SSC does not reduce the amplitudes of the harmonics, care should be taken when studying the influence of the harmonic noise on wireless systems. As a final note, we would like to express our sincere gratitude to those in the Communication Environmental Engineering Section, including Professor Akira Sugiura of the Research Institute of Electrical Communication at Tohoku University, for their collaboration in discussions.

### *References*

1 A. Ogata, Y. Matsumoto, K. Fujii, and A. Sugiura, “Measurement of Radiated Noises from Personal Computers in the WLAN Frequency Band”, Proc. 2004 Asia-Pacific Radio Science Conference, pp. 508-509.

2 K. B. Hardin, J. T. Fessler, and D. R. Bush, “Spread Spectrum Clock Generation for the Reduction of Radiated Emissions”, Proc. 1994 IEEE International Symposium on EMC, pp. 227-231.

3 J. Kim, D.G. Kam, and J. Kim, “Spread Spectrum Clock Generator with Delay Cell Array to Reduce the EMI from a High Speed Digital System”, Proc. 2004 IEEE International Symposium on EMC, pp. 820-825.

4 I. Belokour, P. Edwards, G. Jacobs, and M. Zaremski, “Approaches to Radiated Emissions Reduction of Powertrain Control Modules”, Proc. 2004 IEEE International Symposium on EMC, pp. 212-217.

5 M. Badaroglu, P. Wambacq, G. Van der Plas, S. Donnay, G. G. E. Gielen, and H. J. De Man, “Digital Ground Bounce Reduction by Supply Current Shaping and Clock Frequency Modulation”, IEEE Trans. Computer- aided Design and Integrated Circuits and Systems, Vol. 24, No. 1, pp. 65-76, 2005.

6 Y. Matsumoto, K. Fujii, and A. Sugiura, “An analytical method for determining the optimal modulating waveform for dithered clock generation”, IEEE Trans. Electromagnetic Compatibility, Vol. 47, No. 3, pp. 577- 584, 2005

7 "Investigation into Possible Effects Resulting From Dithered Clock Oscillators on EMC Measurements and Interference to Radio Transmission Systems", Radiocommunications Agency, London U.K., RA REF: AY3377(510001891), 2000, http://www.ofcom.org.uk/static/archive/ra/topics/research/topics/emc/ay3377/ay3377r5.doc.

8 K. B. Hardin, R. A. Oglesbee, and F. Fisher, "Investigation into Interference Potential of Spread-Spectrum Clock Generation to Broadband Digital Communications", IEEE Trans. on EMC, Vol. 45, No. 1, pp. 10-21, 2003.

9 "Further work into the potential effect of the use of dithered clock oscillators on wideband digital radio services", Radiocommunications Agency, London, U.K., Final report AY4092, 2002, http://www.ofcom.org.uk/static/archive/ra/topics/research/topics/emc/finalreport-dco_2.pdf

10 M. Stecher, "Possible Effects of Spread-Spectrum-Clock Interference on Wideband Radiocommunication Services", Proc. 2005 IEEE International Symposium on EMC, TU-AM-3-1.

11 O. Aoki, F. Amemiya, A. Kitani, and N. Kuwabara "Investigation of interferences between wireless LAN signal and disturbances from spread spectrum clocking", Proc. 2004 IEEE International Symposium on EMC, pp. 505-510.

12 T. Shimizu, Y. Matsumoto, K. Fujii, and A. Sugiura, "Performance Evaluation of IEEE802.11a WLAN Interfered by Spread Spectrum Noises from a PC Clock System", IEEE 2005 International Symposium on Microwave, Antenna, Propagation and EMC Technologies For Wireless Communications, pp. 1529-1532, Beijing, Aug. 8-12, 2005.

13 T. Murakami, Y. Matsumoto, K. Fujii, and A. Sugiura, "Interference in the Bluetooth wireless systems caused by electromagnetic disturbances from spread spectrum clock systems", EMC Europe Workshop 2005 Electromagnetic Compatibility of wireless Systems, pp. 399-402, Rome, Sep. 19-21, 2005.

14 Y. Matsumoto, M. Takeuchi, K. Fujii, A. Sugiura, and Y. Yamanaka, "A Time-Domain Microwave Oven Noise Model for the 2.4 GHz Band", IEEE Trans. on EMC, Vol. 45, No. 3, pp. 561-566, 2003.

15 Y. Matsumoto, K. Fujii, and A. Sugiura, "Effects of Spread Spectrum Clocking on Measured Noise Spectra", EMC Europe Workshop 2005 Electromagnetic Compatibility of wireless Systems, pp. 9-12, Rome, Sep. 19-21, 2005.

***MATSUMOTO Yasushi**, Dr. Eng.*

*Group leader, Communications system EMC group, Wireless Communications Department*

*Electromagnetic Compatibility, Wireless Communications*

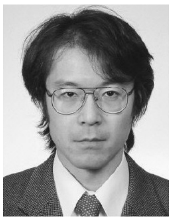

***ISHIGAMI Shinobu**, Dr. Eng.*

*Senior Researcher, EMC Measurement Group, Wireless Communications Department*

*Electromagnetic Compatibility*

***GOTOH Kaoru**, Dr. Eng.*

*Researcher, EMC Measurement Group, Wireless Communications Department*

*Electromagnetic Compatibility, Wireless Communications*